ACS OMEGA

Open Access

http://pubs.acs.org/journal/acsodf

Article

Stretchable Composite Films Are Prepared by Using Cellulose Pulp with Differential Substitution of Carboxymethyl Cellulose and Thymol with an Infrared Heating Process for Packaging Application

Balasubramanian Rukmanikrishnan,*[,†] Chaehyun Jo,[†] Juwon Chae, Sam Soo Kim,* and Jaewoong Lee*

Cite This: *ACS Omega* 2024, 9, 41258−41267

Read Online

ACCESS | Metrics & More | Article Recommendations | Supporting Information

ABSTRACT: Herein, cellulose pulp (CP), carboxymethyl cellulose (CMC), and thymol-based eco-friendly, transparent, and flexible composite films are prepared. These materials dissolved well in an environment-friendly process in *N*-methyl morpholine *N*-oxide (NMMO) ionic liquids using infrared heating. Fourier-transform infrared spectroscopy (FT-IR), X-ray diffraction (XRD), and scanning electron microscopy (SEM) analyses are used to study the structure, microstructure, and morphology of the composite films. The thermal properties of the CP/CMC/thymol composites are thoroughly studied by thermogravimetric analysis (TGA) and differential scanning calorimetry (DSC). The thermal stability of the composites ($T_{5\%}$—57.8−91.2 °C and $T_{10\%}$—216.6−284.1 °C) significantly improves following the CMC addition. In each case, all the composite film exhibits unique T_g (140.5−143.1 °C) values, as confirmed by DSC. The tensile strength of the cellulose pulp is 66.5 MPa, increasing to 78.4 MPa for the CP/CMC-1:0.5 composites and steadily increasing to 93.8 MPa with increasing CMC content. Similarly, CMC increases the EB of cellulose pulp from 9.3 to 7.4%. The water vapor permeability and swelling ratio values of the CP/CMC/thymol composites are in the range of 1.9−2.11 × 10^{-9} g/(m^2·Pa·s) and 52.5−50.8° respectively. The CP, CMC, and thymol-based composite do not exhibit cytotoxicity to the aneuploid immortal keratinocyte cell line and demonstrate excellent antioxidant properties, for promising packaging and biomedical applications.

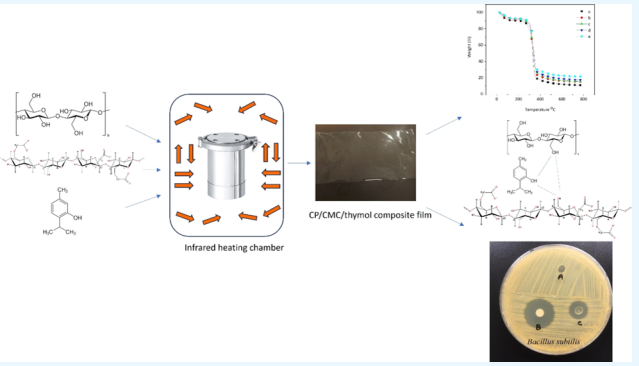

1. INTRODUCTION

Packaging materials derived from nonrenewable petroleum resources and synthetic plastics constitute environmental, health, and toxicity issues, owing to their nonbiodegradability. These concerns and challenges have led to the development of novel environment-friendly and biodegradable packaging materials. Biomass-based nanocomposites are novel composites consisting of biodegradable biopolymers and bionanofillers.[1−3] They are promising renewable resources addressing serious environmental problems, which can also improve the poor mechanical and thermal properties of existing materials. Today, cellulose-based composite films are considered important for packaging, owing to their excellent transparency, mechanical properties, nontoxicity, high biodegradability, and low economic cost, compared with synthetic polymers.[3−9]

Cellulose is the most abundant natural organic molecule on Earth (constituting more than 50% of the total biomass weight). Due to this, it is of great interest to the chemical industry. There has been a strong desire to develop novel polymers based on renewable resources that will compete with synthetic polymers.[10,11] Cellulose pulp is a renewable and affordable raw material, widely used in paper and agro-industries. Carboxymethyl cellulose (CMC) is among the most common derivatives of cellulose, used for preparing edible films. CMC is a linear, long-chain, water-soluble, and anionic polysaccharide, and its solution is highly viscous, nontoxic, and nonallergenic. Additionally, CMC has a lot of hydroxyl and carboxyl groups, which have a good affinity to paper materials and work well as an effective carrier of antibacterial agents. Conventionally, to improve the properties of composite films and expand their function, a variety of materials were added to the CMC film, such as starch/nisin, xanthan gum/polygonatum cyrtonema, hydroxyethyl cellulose (HEC)/nano zinc, poly(vinyl alcohol) (PVA), and silica nanoparticles loaded with caffeic acid to optimize the performance of cassava starch.[12−18]

Most of the previous studies have focused on hydrophilic cellulose films, which are moisture-sensitive owing to the presence of numerous hydrophilic hydroxyl groups. The absorption of moisture results in swelling, reduced strength

Received: March 31, 2024
Revised: August 29, 2024
Accepted: September 3, 2024
Published: September 23, 2024

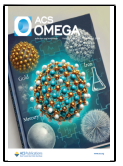

and stiffness, and higher water/air permeability of these films, restricting their usage in high-moisture environments. Therefore, it is critical to overcome this demerit. A chemical modification of cellulose can effectively resolve this issue but those methods often require heating, long reaction times, and catalysts. Further, hydrophobic modification is inefficient and its scale-up is difficult.[19−24]

Along with purity, the degree of substitution (DS), which averages 58 hydroxyl groups replaced with carboxymethyl groups per anhydroglucose unit, has a significant impact on the characteristics and hence the potential uses of CMC. By efficiently reducing the number of hydroxyl groups in cellulose, acetylation can increase the hydrophobicity of the material and decrease the number of H bonds. The kind and quantity of ester groups linked to the chain determine the physical characteristics of cellulose esters. The material properties of cellulose derivatives, in particular their thermal characteristics, hydrophobicity, transparency, processability, and solubility, are greatly influenced by changes in DS. This behavior is very different from that of natural cellulose, which is challenging to treat and does not dissolve in common solvents.[25−28]

Ionic liquids are also very promising for processing cellulose into value-added products, such as fibers and films. They offer several advantages over existing processes, such as averting the emission of volatile organic or toxic compounds in a viscous process, and higher thermal stability than *N*-methyl morpholine *N*-oxide (NMMO), a solvent used in the commercial Lyocell process. However, the recyclability of ionic liquids has not been fully characterized yet, and the development of energy- and cost-efficient recycling strategies remains uncertain.[29−34]

Recently, Natural phenolic compounds have been used extensively in the food industry because of their important antibacterial roles and antioxidant activities. Due to its antibacterial and antioxidant properties, thymol, one of the most prevalent components of thyme and oregano essential oils, has drawn a lot of attention. It is found in the essential oil of the species Cinnamomum. It is a physiologically active substance that gives cinnamon its distinct flavor and aroma and is also a potent inhibitor of bacterial, yeast, and filamentous development.[35−39] Those materials are particularly useful in emerging technologies because they have better structural integrity, barrier properties, and antimicrobial and antioxidant properties. The incorporation of active substances with antioxidant and antimicrobial properties transforms active biological nanocomposites, which are structured hybrid materials created by combining matrices, into biodegradable polymers.

The objective of this study is to develop high-performance active biological nanocomposites based on cellulose pulp for sustainable packaging applications. For this, active compounds were selected and thymol was incorporated into cellulose pulp/CMC composites via a sustainable process.[40−42] We used an infrared heating machine that processed at low temperatures and reduced time to compare with our previous studies.[43,44] In this study, a synergistic combination of cellulose pulp (CP)/CMC/thymol-based composites was prepared through simple dissolution in the NMMO solvent. This unexplored sustainable composite was thoroughly studied by Fourier-transform infrared spectroscopy (FT-IR), X-ray diffraction (XRD), scanning electron microscopy (SEM), and ultraviolet (UV) analyses. The thermal, mechanical, and water-barrier properties are systematically investigated and discussed. Moreover, the antimicrobial activity, antioxidant activity, and cytotoxicity of the prepared CP/CMC/thymol composites were examined. This study provides important guidelines for packaging applications.

2. EXPERIMENTAL SECTION

2.1. Materials. Cellulose pulp composed of α-cellulose (96.0%), hemicellulose (3.8%) and lignin (0.2 wt %) and carboxymethyl cellulose (molecular weight, $M_v \sim 1{,}300{,}000$) were purchased from Moorim P&P Co., Ltd., (South Korea) and Sigma-Aldrich (South Korea), respectively. NMMO (99.0%) and thymol (99.5%) were purchased from Dajang Chemicals (South Korea). A water-soluble tetrazolium salt (WST-1, 98.0%) cat. No #EZ-1000 cytox was purchased from Daeil Lab Service Co. (Seoul, Republic of Korea), for measuring cytotoxicity. All the reagents in this study were used as received.

2.2. Preparation of Cellulose Pulp/Carboxymethyl Cellulose/Thymol Composite Films. CP (4 g), CMC (0.15 of DS) (4 g), and thymol (10 wt %) were mixed using a hand blender. The CP/CMC/thymol mixture was dispersed in a stainless-steel cup NMMO (92 g) and heated to 75 °C in an infrared heating machine. The metal pot was rotated 360° continuously at 400 rpm for 60 min, ensuring even mixing. The infrared heating system helped the stainless-steel cup to avoid the NMMO recrystallization and solvent loss, thereby saving energy, cost, and time. The stainless steel cup was removed after 60 min and maintained in a vacuum oven at 75 °C for 6 h to eliminate air bubbles. Then, a glass plate's surface was evenly coated with the viscous CP/CMC/thymol solution that had been heated to 75 °C. The water on the glass plate was replenished with fresh water every hour, without disrupting the film, in a coagulation bath for 6 h. The CP/CMC/thymol composite film was free of solvent before being transferred to a dried glass plate and allowed to air-dry for 48 h. The produced translucent film has a thickness of about 0.02−0.40 mm.

After 60 min, the stainless-steel cup was removed and kept in a vacuum oven for 6 h at 75 °C, to remove air bubbles. Then, the viscous solution of CP/CMC/thymol at 75 °C was uniformly spread on the surface of a glass plate. The glass plate was immediately placed in a coagulation bath containing water for 6 h; the water in the bath was replaced with fresh water every 1 h, without disturbing the film. The solvent was completely removed from the CP/CMC/thymol composite film, which was transferred to a dried glass plate and dried at room temperature for 48 h. The thickness of the obtained transparent films was in the range of 0.02−0.40 mm. The samples of composite films based on CP with different degrees of substitution of CMC and thymol in the ratio of neat CP, CP/0.15 DS of CMC-1:1, CP/0.20 DS of CMC-1:1, CP/0.25 DS of CMC-1:1, and CP/0.20 DS of CMC-1:1 with 10 wt % of thymol were prepared. The Supporting Information Section contains information on the characterization techniques used for these composite films.

3. RESULTS AND DISCUSSION

3.1. FT-IR. Figure 1 illustrates the structural conformation of the cellulose pulp/CMC and thymol-based composites. Similar characteristic peaks were observed for CP and CMC, owing to the structural backbone. The −CH symmetrical and O−H stretching vibrations of the composite films were observed at 2890 and 3010−3550 cm^{-1}, respectively. Addi-

https://doi.org/10.1021/acsomega.4c03087
ACS Omega 2024, 9, 41258−41267

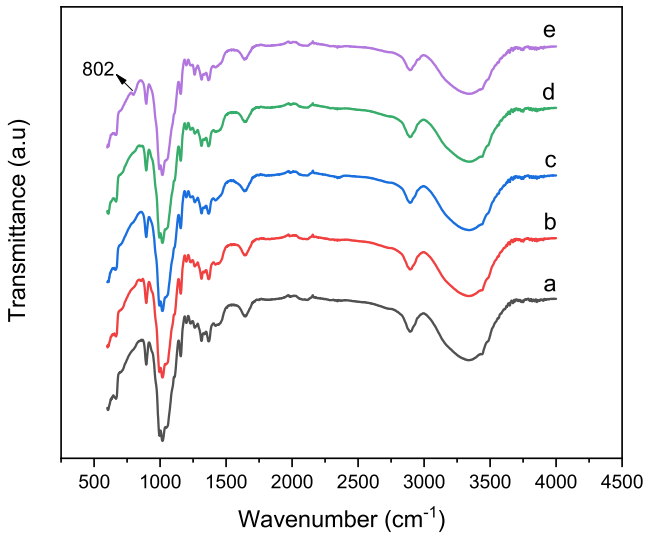

Figure 1. FT-IR spectra of (a) CP, (b) CP/0.15 DS of CMC-1:1, (c) CP/0.20 DS of CMC-1:1, (d) CP/0.25 DS of CMC-1:1, and (e) CP/0.25 DS of CMC-1:1 with 10 wt % of thymol.

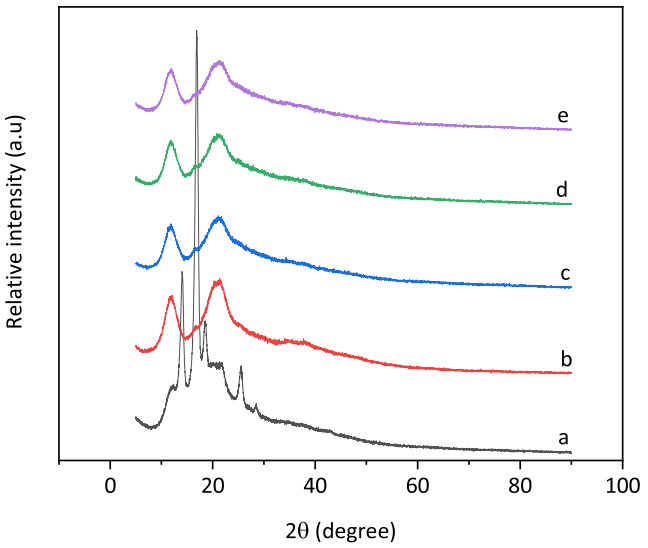

Figure 2. XRD patterns of (a) CP, (b) CP/0.15 DS of CMC-1:1, (c) CP/0.20 DS of CMC-1:1, (d) CP/0.25 DS of CMC-1:1, and (e) CP/0.25 DS of CMC-1:1 with 10 wt % of thymol.

tional peaks were attributed to $-CH_2$ symmetrical bending (1418 cm^{-1}), cellulose C−O−C bridges (1156 cm^{-1}), C−O bond stretching (1056 cm^{-1}), ether C−O−C functionalities (1016 cm^{-1}), and a band at 896 cm^{-1} was observed, which was attributed to β-linked glucose polymers. The CMC substitution yielded an extra absorption band at 1644 cm^{-1}, attributed to the stretching vibration of the introduced carboxylate groups (COO^-). The modified band intensities corresponded to the stretching vibrations of alkyl and OH groups, respectively. The characteristic intense novel peak at 998 cm^{-1} appeared, owing to the asymmetric C−O−C stretching vibration. The characteristic intensity increased for the 890 and 992 cm^{-1} peaks and decreased for the 1151 and 1018 cm^{-1} peaks associated with the C−O and −C−O−H− groups, respectively. In the case of the cellulose pulp/CMC/thymol-based composites, the characteristic peaks observed at 802 cm^{-1} were attributed to aromatic C−H of thymol groups. Nevertheless, some other thymol characteristic peaks were masked by the cellulose bands. These results suggest that H-bond interactions were present in the CP/CMC/thymol composite films.[37−39]

3.2. XRD. The XRD patterns of the cellulose samples with different degrees of CMC and thymol composite films are shown in Figure 2. The characteristic diffraction peaks at 2θ of 14.07, 18.59, 16.87, 25.49, and 28.51° were assigned to the neat CP. The addition of different-DS CMC to CP altered the CP crystal structure. The CP/CMC composites exhibited two different diffraction peaks at 2θ of 11.87 and 21.05°. The addition of CMC significantly altered the CP crystallinity structure. The peak intensity decreased with increasing CMC in CP/CMC (high DS). This occurred because a reduction of the cellulose crystallinity deteriorated its reinforcing efficiency. These results indicate that intermolecular interactions are mainly present in the surface and amorphous layers and do not strongly affect the inner crystalline structure of cellulose.[4,5] The addition of thymol did not affect the CP/CMC structure. The crystallinity or the XRD pattern of the CP samples with different DS values of CMC composite films were fairly close, with peaks at 11.87 and 21.05°, indicating that the DS did not significantly affect the crystal and chemical structure of the composite films.

3.3. UV/Color. The UV transmission characteristics of the CP/CMC/thymol composites are shown in Figure 3 and

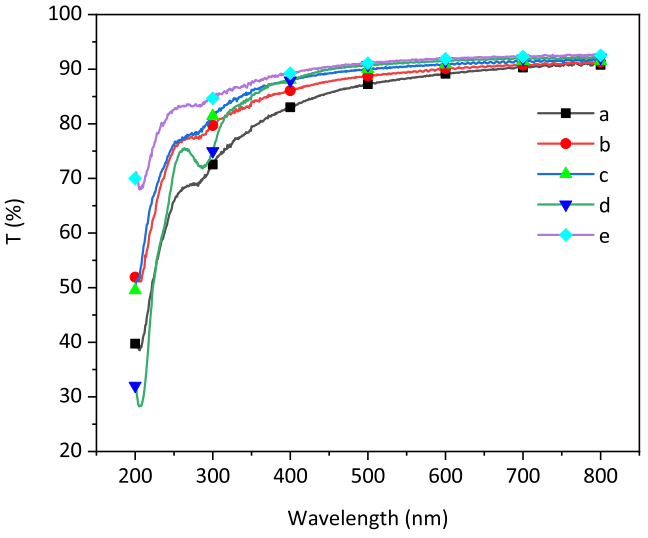

Figure 3. UV transmittance spectra of (a) CP, (b) CP/0.15 DS of CMC-1:1, (c) CP/0.20 DS of CMC-1:1, (d) CP/0.25 DS of CMC-1:1, and (e) CP/0.25 DS of CMC-1:1 with 10 wt % of thymol.

Table 1. The light transmittance for the neat CP composite films was 89.1% at 600 nm. The transmittances of the CP composite films increased to 90.1, 90.9, 91.5, and 92%, for the CP/0.15 DS of CMC-1:1, CP/0.2 DS of CMC-1:1, CP/0.25 DS of CMC-1:1, and CP/0.25 DS of CMC-1:1 with 10 wt % of thymol composites. The addition of different-DS CMC improved the transparency of the films by 50%, compared with the neat CP film. Furthermore, the transparency did not change significantly with the incorporation of thymol into the CP/CMC composite films. Overall, the transmittances of the prepared composite films were better than the reported values

https://doi.org/10.1021/acsomega.4c03087
ACS Omega 2024, 9, 41258−41267

Table 1. Thickness, UV-Spectra, and Color Properties of CP, CMC, and Thymol-Based Composite Films

samples	thickness (mm)	T (%) at 600 nm	lightness (L^*)	redness (a^*)	yellowness (b^*)
CP	85.08 ± 0.82	2.67 ± 0.11	−5.03	0.07	9.3
CP/0.15 DS of CMC-1:1	83.98 ± 0.46	2.54 ± 0.15	−4.41	0.08	14.3
CP/0.2 DS of CMC-1:1	84.44 ± 0.47	2.62 ± 0.22	−4.05	0.09	18.9
CP/0.25 DS of CMC-1:1	84.81 ± 0.46	2.41 ± 0.19	−4.61	0.08	23.5
CP/0.25 DS of CMC-1:1 with 10 wt % of thymol	84.68 ± 0.24	2.27 ± 0.29	−3.63	0.09	23.1

Table 2. Water Vapor Permeability, Contact Angle Swelling Ratio, and Mechanical Properties of CP, CMC, and Thymol Based Composite Films

samples	water vapor permeability ($\times 10^{-9}$ g/m^2·Pa·s)	water contact angle (deg)	swelling ratio (%)	tensile strength (MPa)	elongation at break (%)
CP	1.90 ± 0.22	52.5 ± 1.3	191 ± 12	66.5 ± 1.5	9.3 ± 0.8
CP/0.15 DS of CMC-1:1	1.82 ± 0.14	51.0 ± 0.9	197 ± 14	78.4 ± 2.3	14.3 ± 0.8
CP/0.2 DS of CMC-1:1	2.04 ± 0.18	51.5 ± 0.8	205 ± 17	84.1 ± 2.1	18.9 ± 1.2
CP/0.25 DS of CMC-1:1	2.26 ± 0.24	50.2 ± 1.5	213 ± 12	88.3 ± 2.7	23.5 ± 1.1
CP/0.25 DS of CMC-1:1 with 10 wt % of thymol	2.11 ± 0.20	50.8 ± 1.1	206 ± 15	93.8 ± 3.0	23.1 ± 0.9

for composite films. Thus, transparent CP/CMC/thymol composite films are suitable for packaging applications.

3.4. Swelling Ratio. The swelling behavior, ability, and capability of the prepared CP/CMC composites were investigated; the results are summarized in Table 2. The SR values for the neat and pure CP composites were 191%. The SR of a polymer composite depends on the cross-linking density, hydrophilicity, and crystallinity of the underlying polymer network. An experiment was conducted in water for different time intervals and periods. The SR values of 197, 205, 213, and 206% were registered for the CP/0.15 DS of CMC-1:1, CP/0.2 DS of CMC-1:1, CP/0.25 DS of CMC-1:1, and CP/0.25 DS of CMC-1:1 with 10 wt % of thymol composites, respectively. Moreover, the SR values decreased slightly to 55%, following the addition of thymol to the prepared CP/CMC composites. The presence of CMC decreased the cross-linking reaction and the crystallinity between the CP/CMC polymer matrix and the polymer chain, thus lowering the SR values of the prepared CP/CMC composites. The high degree of swelling in the CP/CMC composites was possibly due to the high CMC hydrophilicity.[45]

3.5. Contact Angle. The surface hydrophobicity of a biopolymer-based composite film is an essential parameter for packaging applications. The surface wettability of the prepared composite films was measured by the CA analysis (Table 2 and Figure S1), which maps the hydrophilic and hydrophobic properties of an analyzed film surface. Among the prepared composites, CP exhibited the lowest CA of 52.5°, owing to its hydrophilic nature. Following the CMC addition (high DS), the CP/CMC composites exhibited the lowest CA values. This may be owing to the substitution of hydroxyl groups by acetyl groups and the corresponding decrease in the cellulose polarity.[26] The incorporation of thymol increased the CA values from 50.2 to 50.8°. This may be attributed to the hydrophobic nature of thymol and the covalent interactions between the CP/CMC and polyphenol compounds present in thymol.

3.6. Water Vapor Permeability. The water barrier properties of biopolymers are important. These properties prevent environmental moisture absorption, thus prolonging the shelf life of the product. The neat CP exhibited the highest WVP value of 1.9×10^{-9} g/m^2·Pa·s. The value was slightly reduced to 1.82×10^{-9} g/m^2·Pa·s for the CP/CMC composites and increased with the addition of high DS of CMC (Table 2). Moreover, the addition of thymol reduced the WVP values from 2.26 to 2.11×10^{-9} g/m^2·Pa·s. Water molecules are repelled owing to the hydrophobic nature of the thymol compound at the optimal concentration. The results of this analysis were consistent with the SEM and CA results. Similar results have been reported regarding the incorporation of thymol-based polymer composites.[32−36]

3.7. Mechanical Properties. The mechanical properties of polymer composites provide insights into their internal structure and are strongly affected by the microstructure of the composites.[10] The tensile strength and break elongation values of the CP/CMC composites are listed in Table 2. The prepared CP/CMC/thymol composites exhibited excellent film-forming ability, transparency, and flexibility. The TS value of the neat composite was 66.5 MPa, which increased to 78.4 MPa following the CMC addition (0.15% DS). The prepared CP/CMC/thymol composites exhibited the highest TS value of 93.8 MPa, which was not significant compared with that for the neat CP composite films. The mechanical properties of cellulose materials depend on many variables, such as the DS of CMC, and the crystallinity of the materials. Consequently, the alignment of the CMC with the CP chain was better for higher-DS CMC and was more improved for higher-DS CMC. However, for higher-DS CMC, increasing the steric hindrance through the attached acetyl groups impaired the alignment of molecules along the molecular axis.[28,29] The EB of the neat CP composite films was 9.3%, decreasing to 14.3, 18.9, 23.5, and 23.1% for CP/0.15 DS of CMC-1:1, CP/0.20 DS of CMC-1:1, CP/0.25 DS of CMC-1:1, and CP/0.25 DS of CMC-1:1 with 10 wt % of thymol composites, respectively. The prepared composite films exhibited considerable mechanical, contact angle, and water resistance properties compared to various composite films (Table S1). The results indicate that the dispersion and compatibility properties of the prepared CP/CMC/thymol composites were good and significantly affected the TS and EB properties of the composites.

3.8. SEM Analysis. The SEM images of the prepared CP/CMC composites revealed the dispersion and surface morphologies of the corresponding polymer matrices. The microscope images of all the composites exhibited smooth, flat shapes without cracks or voids. The addition of CMC and thymol does not alter the CP morphology and dispersal

https://doi.org/10.1021/acsomega.4c03087
ACS Omega 2024, 9, 41258−41267

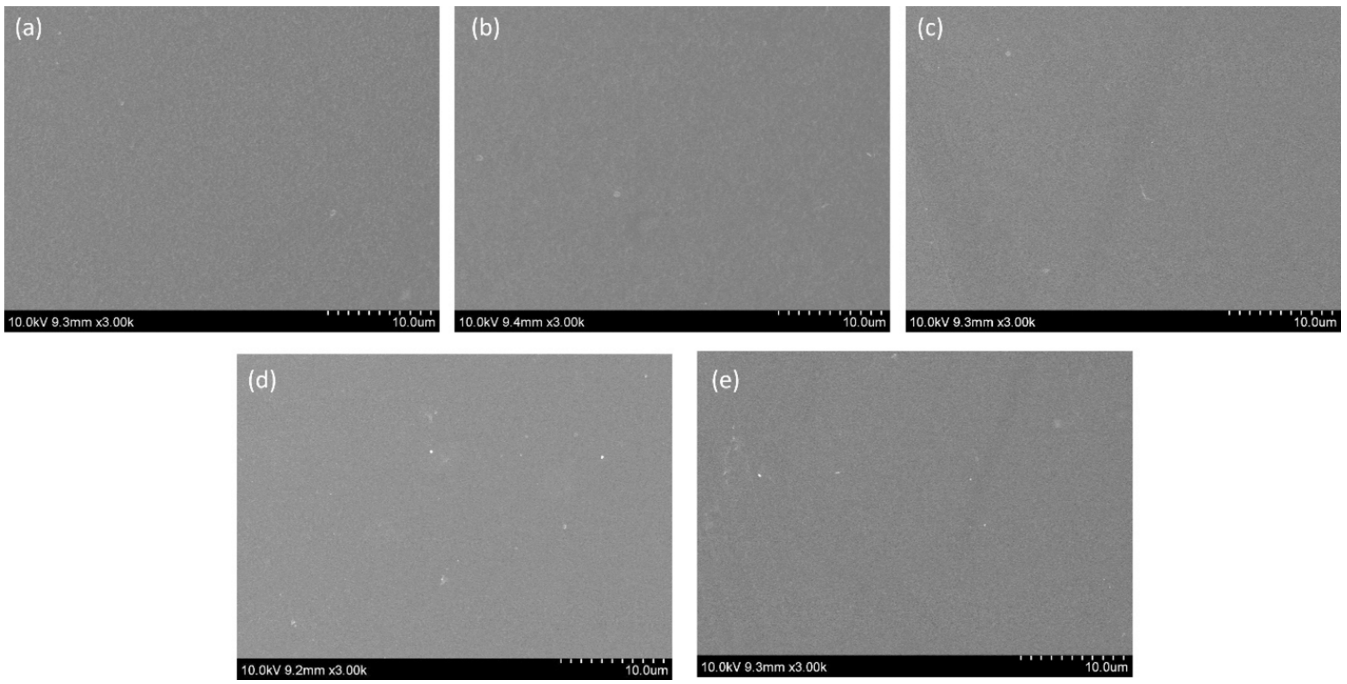

Figure 4. SEM images of (a) CP, (b) CP/0.15 DS of CMC-1:1, (c) CP/0.20 DS of CMC-1:1, (d) CP/0.25 DS of CMC-1:1, and (e) CP/0.25 DS of CMC-1:1 with 10 wt % of thymol.

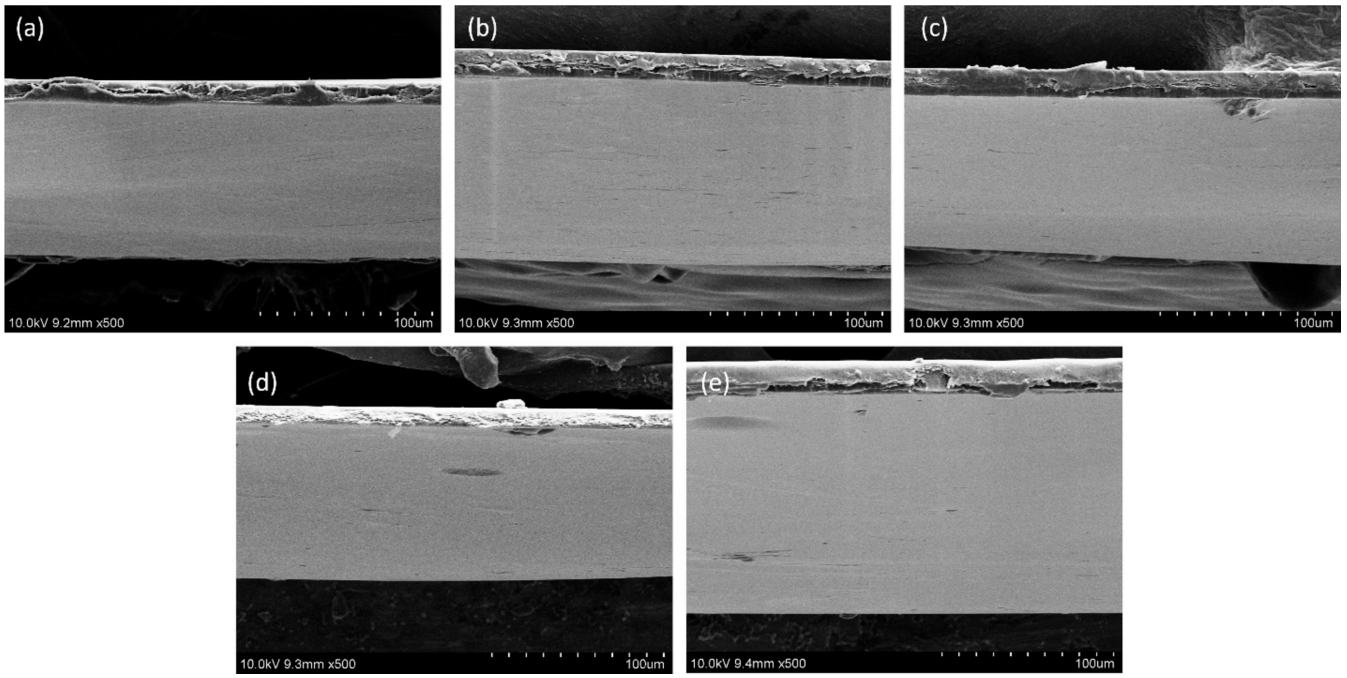

Figure 5. Cross-section SEM images of (a) CP, (b) CP/0.15 DS of CMC-1:1, (c) CP/0.20 DS of CMC-1:1, (d) CP/0.25 DS of CMC-1:1, and (e) CP/0.25 DS of CMC-1:1 with 10 wt % of thymol.

homogeneity on the surfaces of the prepared CP/CMC/thymol composites, as shown in Figures 4 and 5. These results are consistent and are confirmed by the cross-sectional images shown in Figure 5. The cross-sectional CP images revealed uneven, slightly rougher, and coarser surfaces without cracks and morphological aggregates. However, the cross-sectional images of the prepared CP/CMC and CP/CMC/thymol composites revealed compact, uniform, and increasingly homogeneous morphologies. The addition of CMC with different DS and thymol components resulted in the formation of homogeneous morphologies. The results showed that all the materials were comparable and exhibited good adhesion between the polymers. This reinforcement effect led to a resistant interface, which enhanced the mechanical properties of the polymer composites.[46]

3.9. TGA. The thermal stability of the prepared CP/CMC/thymol composites was investigated; the data are summarized in Table 3 and Figure 6. The 5 and 10% gravimetric losses of the prepared composites were in the range of 57.8−91.2 and 216.6−284.1 °C, respectively. The initial degradation step was

https://doi.org/10.1021/acsomega.4c03087
ACS Omega 2024, 9, 41258−41267

Table 3. Thermal Properties of CP, CMC, and Thymol-Based Composite Films

samples	TGA			DSC	
	$T_{5\%}$	$T_{10\%}$	CY (%)	T_g (°C)	T_m (°C)
CP	57.8	216.6	12.0	140.5	186.1
CP/0.15 DS of CMC-1:1	69.4	266.5	16.3	142.8	186.4
CP/0.2 DS of CMC-1:1	82.4	267.8	17.1	144.2	190.1
CP/0.25 DS of CMC-1:1	90.1	282.6	18.8	142.6	192.5
CP/0.25 DS of CMC-1:1 with 10 wt % of thymol	91.2	284.1	22.6	143.1	196.3

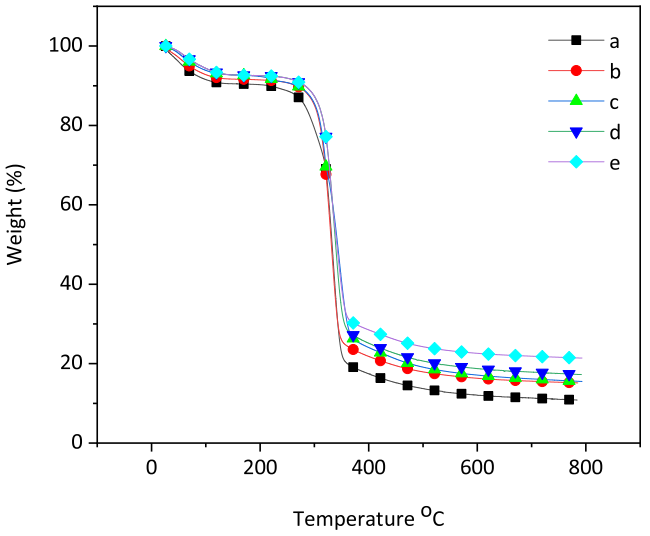

Figure 6. TGA curves of (a) CP, (b) CP/0.15 DS of CMC-1:1, (c) CP/0.20 DS of CMC-1:1, (d) CP/0.25 DS of CMC-1:1, and (e) CP/0.25 DS of CMC-1:1 with 10 wt % of thymol.

likely due to the presence of labile oxygen-containing functional groups on the CP, CMC, and thymol components, which were lost at temperatures ranging from 50 to 130 °C. The CMC addition significantly improved the initial degradation temperatures of the composites. A trend toward increasing thermal stability was observed following the CMC incorporation into the CP chains. The higher-DS CMC exhibited excellent thermal stability, even compared with neat CP, while the CMC incorporation increased the amount of thermally labile oxygen functionalities. However, the thermal behavior and the low DS of CMC may also indicate that the sample had a smaller amount of CMC attached to the CP backbone, leading to its distinctive thermal stability. The covalently linked CMC is assumed to be homogeneously distributed on the polymer backbone, forming thermally insulating CMC layers, which could increase the thermal stability of the composite films. The residual chars of the composites increased following the addition of different DSs of CMC and thymol. The amount of residual char commonly increases for the composites loaded with different polymeric materials. It has also been suggested that the interactions between the CP and CMC materials lead to higher char residues.

3.10. DSC. The DSC thermograms of the CP and CP/CMC/thymol composites were studied; the data are presented in Table 3. The neat CP and CMC-added CP composites exhibited clear glass transition temperatures (T_g) and melting temperatures (T_m), as typically observed for thermoplastic products. The plain CP specimen exhibited T_g of 140.5 °C, while for different DS of CMC loadings the T_g values shifted to 142.8, 144.2, 142.6 and 143.1 °C, respectively for CP/0.15 DS of CMC-1:1, CP/0.20 DS of CMC-1:1, CP/0.25 DS of CMC-1:1, and CP/0.25 DS of CMC-1:1 with 10 wt % of thymol. The prepared CP/0.25 DS of CMC-1:1 with 10 wt % of thymol composites exhibited the highest T_g, owing to the good

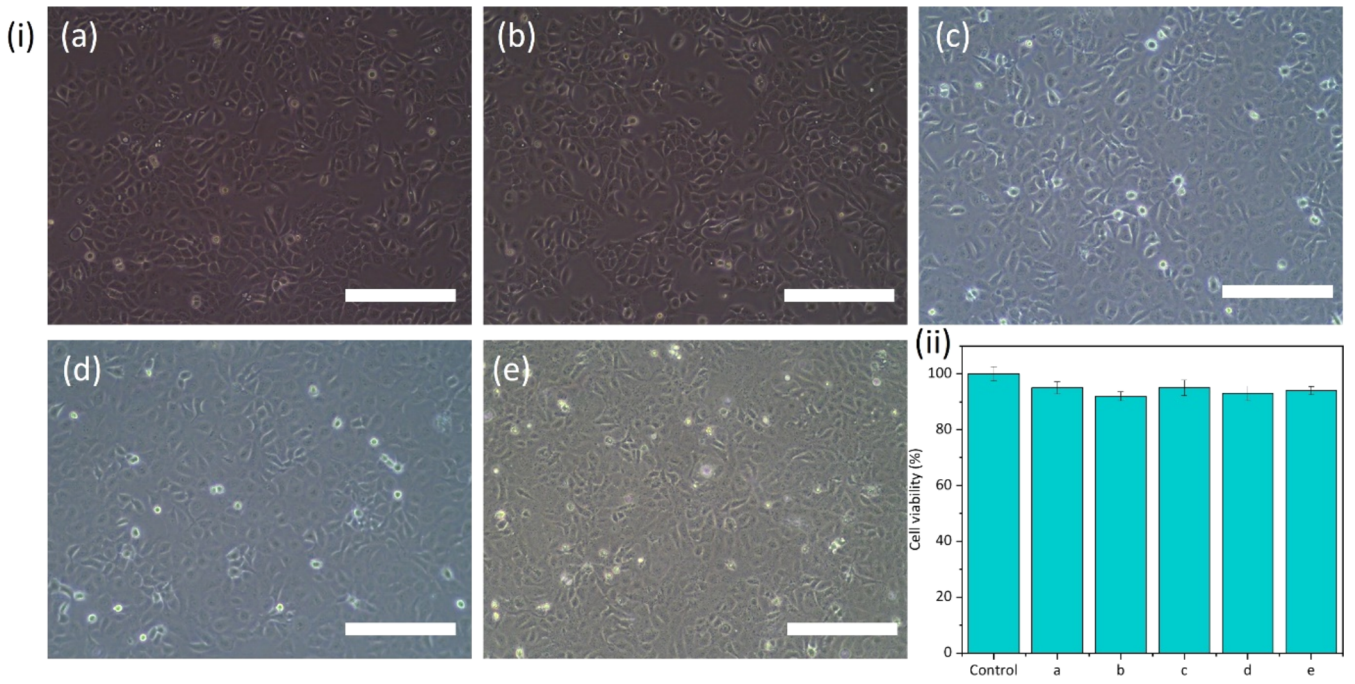

Figure 7. (i) Light microscopy images and (ii) cell viability of HaCaT cell line of (a) CP, (b) CP/0.15 DS of CMC-1:1, (c) CP/0.20 DS of CMC-1:1, (d) CP/0.25 DS of CMC-1:1, and (e) CP/0.25 DS of CMC-1:1 with 10 wt % of thymol (scale bars are 100 μm).

https://doi.org/10.1021/acsomega.4c03087
ACS Omega 2024, 9, 41258−41267

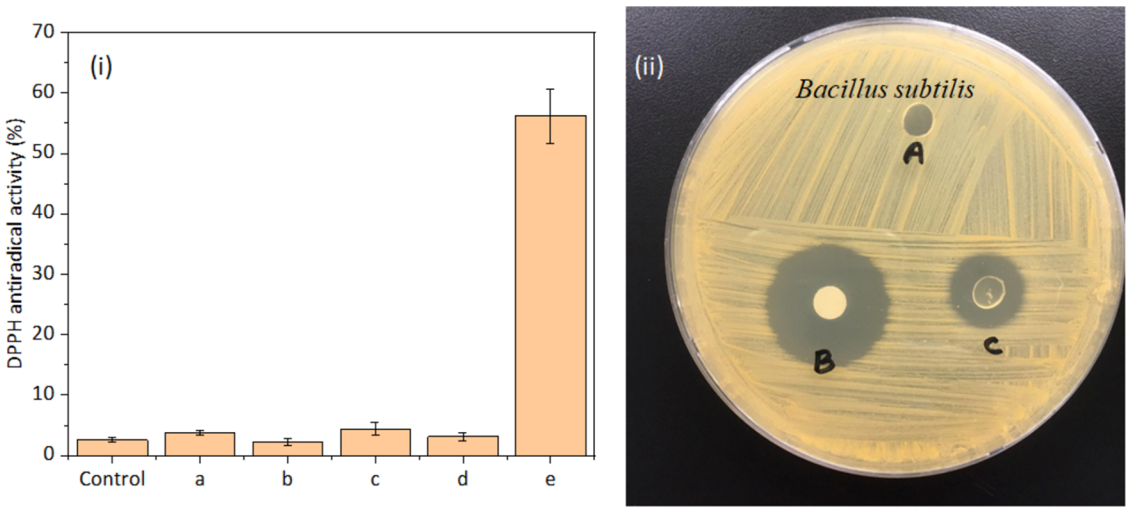

Figure 8. (i) DPPH radical scavenging activity of (a) CP, (b) CP/0.15 DS of CMC-1:1, (c) CP/0.20 DS of CMC-1:1, (d) CP/0.25 DS of CMC-1:1, and (e) CP/0.25 DS of CMC-1:1 with 10 wt % of thymol; (ii) representative images showing the antibacterial activity of (a) A—negative control (sterile distilled water in the agar well method and untreated composite film (CP/CMC/thymol) in the disc method), B—positive control (10 μg of ciprofloxacin), and C—CP/0.25 DS of CMC-1:1 with 10 wt % of thymol composite film against *Bacillus subtilis*.

polymer−filler interaction. This may be explained by the interaction of the polymers with the filler particles, which decreased the flexibility and molecular mobility of the polymer chains. As a result, a relatively high temperature was needed to change the polymer from its glassy form to its rubbery state. The T_m value of plain CP was 186.1 °C, and following the addition of CMC, this value significantly rose to 196.3 °C. This rise could be explained by the development of cross-linked structures and increased compatibility, which serve as crystal growth's nucleating sites. This effect might be brought on by the rise in cross-linked structures between CP and CMC, which decreased the mobility of the amorphous polymer chains while enhancing interfacial compatibility.[10,29,31,35]

3.11. Cytotoxicity. The cytotoxicity of the CP, CP/CMC, and CP/CMC/thymol composite films were studied using the WST-1 assay on human keratinocyte cells (HaCat cell line); the results are summarized in Figure 7. There was no significant difference between the results for the control cells, across all the studied CP and CP/CMC composite films. However, the prepared CP, CP/CMC, and CP/CMC/thymol composites exhibited only a very slight decrease in cell viability compared to the control group. None of the five composite films had any effect on the incubation medium. The cells showed relatively high activity and proliferation ability in the case of the thymol-loaded composite films. These findings indicate that cellulose pulp and CMC-based composites did not detrimentally affect HaCat cells, suggesting that these composites are safe to use in food and biomedical applications. Summarizing the results obtained for the HaCat cells treated with the new derivatives (compared with the parent substances), we concluded that only the CP/CMC/thymol derivative exhibited the lowest inhibiting capacity, making this derivative attractive as an efficient antioxidant with negligible cytotoxic effects.[47,48]

3.12. Antioxidant Properties. Biopolymer-based composite sheets for packaging applications have antioxidant properties that reveal information about the product's shelf life as well as its aesthetic and nutritional aspects without compromising its integrity. A well-known antioxidant, thymol exhibits good antioxidant activity in polymer composites when measured by the suppression of the DPPH radical (Figure 8i). The levels of thymol that are still present in the polymer matrix, which can function as an active (antioxidant) agent, are shown by the inhibition values. In addition, while creating and using these biological nanocomposites, thymol can shield the polymer matrix from oxidative deterioration. The results of the evaluation of the DPPH radical scavenging abilities of the CP, CP/CMC, and CP/CMC/thymol composites are displayed in Figure 8a. As anticipated, neither the pure cellulose pulp nor the CP/CMC composites showed any antioxidant activity. The CP/CMC/thymol composite, on the other hand, demonstrated good antioxidant activity at 56.2% for 1 h incubation durations, respectively. Thymol has better antioxidant activity as measured for lipids than carvacrol because it has more phenolic steric hindrance. It is well-known that substances like BHT, which have their hydroxyl groups sterically inhibited, have strong antioxidant properties. DPPH radicals are reduced by eugenol and BHT even if only one hydrogen is present in the hydroxyl group. To explain the antiradical efficacies of various monophenolic compounds, some theories have been put forth. As a result, CP/CMC/thymol composites are attractive materials for packaging applications due to their antioxidant capabilities.[47,48]

3.13. Antimicrobial Properties. The antimicrobial properties of the CP, CP/CMC, and CP/CMC/thymol composites were studied using the good diffusion method; the results for their inhibition zones are listed in Table S2 and Figure 8ii. This study was broadly performed using Gram-positive (*Staphylococcus aureus*, *Bacillus cereus*, *Listeria monocytogenes*, and *Bacillus subtilis*) and Gram-negative (*Salmonella typhi* and *Cronobacter sakazakii*) pathogens. As expected, the neat CP and CP/CMC composites had no considerable antimicrobial effect on these bacteria. However, following the incorporation of thymol, the composites exhibited relatively high antimicrobial activity against both Gram-positive and Gram-negative bacteria. The CP/CMC/thymol composite exhibited a high antimicrobial inhibition zone against the *S. aureus* strain (17.1 mm) and weaker activity against the *B. cereus* strain (10.3 mm). The addition of thymol significantly improved the antimicrobial properties of CP/CMC/thymol

https://doi.org/10.1021/acsomega.4c03087
ACS Omega 2024, 9, 41258−41267

composites and extended their potential scope of use in packaging. It is quite likely that the presence of an extra outer membrane, which prevents the dispersion of hydrophobic substances across the cytoplasmic membrane, contributes to the relatively high resistance of Gram-negative bacteria to CP/CMC-thymol. Thymol's antibacterial properties are mostly linked to its active ingredients, eugenol and other hydrophobic chemicals, which can penetrate cell walls and membranes to destroy cellular structures and cause cell death. Additionally, thymol prevents the production of cellular proteins necessary for cell growth as well as the replication of DNA.

4. CONCLUSIONS

Cellulose pulp, CMC, and thymol dissolved well in the ionic liquid NMMO without any fine particles; the resultant solutions had good stability and fluidity. The CP/CMC/thymol composite films were fabricated and characterized. The structure and morphology of the composites confirmed by the FT-IR, XRD, and SEM analyses demonstrated that the incorporation of CMC significantly influenced the cellulose pulp matrix. The prepared composite films' apparent color and UV transmittance properties were not significantly affected by the CMC addition. CMC in the prepared CP/CMC/thymol composites increased the initial thermal degradation temperature of the cellulose pulp from 57.8−91.2 °C. The T_g value of the composite slightly increased from 140.5 to 143.1 °C, as confirmed by DSC. The strong and brittle nature of the cellulose pulp films was significantly modified by CMC as an elastic and flexible CP/CMC composite film. The EB values of the composites decreased by 152%. The CP/CMC and CP/CMC/thymol composites exhibited good WVP ($1.90−2.11 \times 10^{-9}$ g/m^2·Pa·s) and SR (191−213%) values. CP/CMC/thymol composites showed excellent antimicrobial activity against Gram-positive (*S. aureus*, *B. cereus*, *L. monocytogenes*, and *B. subtilis*) and Gram-negative pathogens (*S. typhi* and *C. sakazakii*). This outstanding multifunctionality, noncytotoxicity concerning the HaCat cell line, and good antioxidant activity make CP/CMC/thymol composites promising for food-packaging applications.

■ ASSOCIATED CONTENT

Supporting Information

The Supporting Information is available free of charge at https://pubs.acs.org/doi/10.1021/acsomega.4c03087.

Characterization methods, table of microbial properties, and references (PDF)

■ AUTHOR INFORMATION

Corresponding Authors

Balasubramanian Rukmanikrishnan − *Department of Fiber System Engineering, Yeungnam University, Gyeongsan 38541, South Korea;* orcid.org/0000-0001-6207-7271; Email: rukmibala@gmail.com

Sam Soo Kim − *Department of Fiber System Engineering, Yeungnam University, Gyeongsan 38541, South Korea;* Email: sskim@yu.ac.kr

Jaewoong Lee − *Department of Fiber System Engineering, Yeungnam University, Gyeongsan 38541, South Korea;* Phone: +82-53-810-2786; Email: jaewlee@yu.ac.kr; Fax: +82-53.810.4685

Authors

Chaehyun Jo − *Department of Fiber System Engineering, Yeungnam University, Gyeongsan 38541, South Korea*

Juwon Chae − *Department of Fiber System Engineering, Yeungnam University, Gyeongsan 38541, South Korea*

Complete contact information is available at: https://pubs.acs.org/10.1021/acsomega.4c03087

Author Contributions

†B.R. and C.J. contributed equally to this work.

Notes

The authors declare no competing financial interest.

■ ACKNOWLEDGMENTS

This work was supported by Korea Institute for advancement of Technology (KIAT) grant funded by the Korea Government (MOTIE) (P0012770).

■ REFERENCES

(1) Casaburi, A.; Rojo, Ú. M.; Cerrutti, P.; Vázquez, A.; Foresti, M. L. Carboxymethyl cellulose with tailored degree of substitution obtained from bacterial cellulose. *Food Hydrocolloids* **2018**, *75*, 147−156.

(2) Kassab, Z.; Syafri, E.; Tamraoui, Y.; Hannache, H.; El Kacem Qaiss, A.; El Achaby, M. Characteristics of sulfated and carboxylated cellulose nanocrystals extracted from Juncus plant stems. *Int. J. Biol. Macromol.* **2020**, *154*, 1419−1425.

(3) Lin, C.; Chen, B.; Liu, Y.; Chen, Y.; Liu, M.; Zhu, J. Y. Carboxylated cellulose nanocrystals with chiral nematic property from cotton by dicarboxylic acid hydrolysis. *Carbohydr. Polym.* **2021**, *264*, No. 118039.

(4) Deng, S.; Huang, R.; Zhou, M.; Chen, F.; Fu, Q. Hydrophobic cellulose films with excellent strength and toughness via ball milling activated acylation of microfibrillated cellulose. *Carbohydr. Polym.* **2016**, *154*, 129−138.

(5) Wang, J.; Chen, X.; Zhang, C.; Akbar, A. R.; Shi, Z.; Yang, Q.; Xiong, C. Transparent konjac glucomannan/cellulose nanofibril composite films with improved mechanical properties and thermal stability. *Cellulose* **2019**, *26*, 3155−3165.

(6) Phinichka, N.; Kaenthong, S. Regenerated cellulose from high alpha cellulose pulp of steam-exploded sugarcane bagasse. *J. Mater. Res. Technol.* **2018**, *7*, 55−65.

(7) Hadi, A.; Nawab, A.; Alam, F.; Naqvi, S. Development of sodium alginate−aloe vera hydrogel films enriched with organic fibers: study of the physical, mechanical, and barrier properties for food-packaging applications. *Sustainable Food Technol.* **2023**, *1*, 863−873.

(8) Bhatia, S.; Shah, Y. A.; Al-Harrasi, A.; Jawad, M.; Koca, E.; Aydemir, L. Y. Enhancing Tensile Strength, Thermal Stability, and Antioxidant Characteristics of Transparent Kappa Carrageenan Films Using Grapefruit Essential Oil for Food Packaging Applications. *ACS Omega* **2024**, *9*, 9003−9012.

(9) Gasti, T.; Dixit, S.; Chougale, R. B.; Masti, S. P. Fabrication of novel gallic acid functionalized chitosan/pullulan active bio-films for the preservation and shelf-life extension of green chillies. *Sustainable Food Technol.* **2023**, *1*, 390−403.

(10) Ashok, B.; Reddy, K. O.; Madhukar, K.; Cai, J.; Zhang, L.; Rajulu, A. V. Properties of cellulose/Thespesia lampas short fibers bio-composite films. *Carbohydr. Polym.* **2015**, *127*, 110−115.

(11) Hu, W.; Chen, G.; Liu, Y.; Liu, Y.; Li, B.; Fang, Z. Transparent and Hazy All-Cellulose Composite Films with Superior Mechanical Properties. *ACS Sustainable Chem. Eng.* **2018**, *6*, 6974−6980.

(12) Lopez, C. G.; Colby, R. H.; Cabral, J. T. Electrostatic and Hydrophobic Interactions in NaCMC Aqueous Solutions: Effect of Degree of Substitution. *Macromolecules* **2018**, *51*, 3165−3175.

(13) Yamakawa, A.; Suzuki, S.; Oku, T.; Enomoto, K.; Ikeda, M.; Rodrigue, J.; Tateiwa, K.; Terada, Y.; Yano, H.; Kitamura, S.

Nanostructure and physical properties of cellulose nanofiber-carbon nanotube composite films. *Carbohydr. Polym.* **2017**, *171*, 129−135.
(14) Lin, L.; Peng, S.; Chen, X.; Li, C.; Cui, H. Silica nanoparticles loaded with caffeic acid to optimize the performance of cassava starch/sodium carboxymethylcellulose film for meat packaging. *Int. J. Biol. Macromol.* **2023**, *241*, No. 124591.
(15) Cen, C.; Wang, F.; Wang, Y.; Li, H.; Fu, L.; Li, Y.; Chen, J.; Wang, Y. Design and characterization of an antibacterial film composited by hydroxyethyl cellulose (HEC), carboxymethyl chitosan (CMCS), and nano ZnO for food packaging. *Int. J. Biol. Macromol.* **2023**, *231*, No. 123203.
(16) Zheng, M.; Su, H.; Xiao, R.; Chen, J.; Chen, H.; Tan, K. B.; Zhu, Y. Effects of *Polygonatum cyrtonema* extracts on the antioxidant ability, physical and structure properties of carboxymethyl cellulose-xanthan gum-flaxseed gum active packaging films. *Food Chem.* **2023**, *403*, No. 134320.
(17) Wu, Y.; Li, C. A double-layer smart film based on gellan gum/modified anthocyanin and sodium carboxymethylcellulose/starch/Nisin for application in chicken breast. *Int. J. Biol. Macromol.* **2023**, *232*, No. 123464.
(18) Lin, Z.; Fu, H.; Zhang, Y.; Deng, Y.; Wei, F.; Li, H.; Xu, C.; Hua, F.; Lin, B. Enhanced antibacterial effect and biodegradation of coating via dual-in-situ growth based on carboxymethylcellulose. *Carbohydr. Polym.* **2023**, *302*, No. 120433.
(19) Komorowska, P.; Różańska, S.; Różański, J. Effect of the degree of substitution on the rheology of sodium carboxymethylcellulose solutions in propylene glycol/water mixtures. *Cellulose* **2017**, *24*, 4151−4162.
(20) Xin, C.; Nie, L.; Chen, H.; Li, J.; Li, B. Effect of degree of substitution of carboxymethyl cellulose sodium on the state of water, rheological and baking performance of frozen bread dough. *Food Hydrocolloids* **2018**, *80*, 8−14.
(21) Freire, C. S. R.; Silvestre, A. J. D.; Neto, C. P.; Gandini, A.; Martin, L.; Mondragon, I. Composites based on acylated cellulose fibers and low-density polyethylene: Effect of the fiber content, degree of substitution and fatty acid chain length on final properties. *Compos. Sci. Technol.* **2008**, *68*, 3358−3364.
(22) Crépy, L.; Chaveriat, L.; Banoub, J.; Martin, P.; Joly, N. Synthesis of Cellulose Fatty Esters as Plastics—Influence of the Degree of Substitution and the Fatty Chain Length on Mechanical Properties. *ChemSusChem* **2009**, *2*, 165−170.
(23) Olonisakin, K.; Li, R.; Zhang, X. X.; Xiao, F.; Gao, J.; Yang, W. Effect of TDI-Assisted Hydrophobic Surface Modification of Microcrystalline Cellulose on the Tensile Fracture of MCC/PLA Composite, and Estimation of the Degree of Substitution by Linear Regression. *Langmuir.* **2021**, *37*, 793−801.
(24) Hashmi, M.; Ullah, S.; Ullah, A.; Saito, Y.; Haider, M. K.; Bie, X.; Wada, K.; Kim, I. S. Carboxymethyl Cellulose (CMC) Based Electrospun Composite Nanofiber Mats for Food Packaging. *Polymers* **2021**, *13*, No. 302.
(25) Zhou, X.; Lin, X.; White, K. L.; Lin, S.; Wu, H.; Cao, S.; Huang, L.; Chen, L. Effect of the degree of substitution on the hydrophobicity of acetylated cellulose for production of liquid marbles. *Cellulose* **2016**, *23*, 811−821.
(26) Asaadi, S.; Kakko, T.; King, A. W. T.; Kilpeläinen, I.; Hummel, M.; Sixta, H. High-Performance Acetylated Ioncell-F Fibers with Low Degree of Substitution. *ACS Sustainable Chem. Eng.* **2018**, *6*, 9418−9426.
(27) Gustavsson, L. H.; Adolfsson, K. H.; Hakkarainen, M. Thermoplastic "All-Cellulose" Composites with Covalently Attached Carbonized Cellulose. *Biomacromolecules* **2020**, *21*, 1752−1761.
(28) Hult, E. L.; Iversen, T.; Sugiyama, J. Characterization of the supermolecular structure of cellulose in wood pulp fibres. *Cellulose* **2003**, *10*, 103−110.
(29) Ninan, N.; Muthiah, M.; Park, I. K.; Elain, A.; Thomas, S.; Grohens, Y. Pectin/carboxymethyl cellulose/microfibrillated cellulose composite scaffolds for tissue engineering. *Carbohydr. Polym.* **2013**, *98*, 877−885.
(30) Lin, N.; Dufresne, A. Surface chemistry, morphological analysis and properties of cellulose nanocrystals with gradiented sulfation degrees. *Nanoscale* **2014**, *6*, 5384−5393.
(31) Dong, F.; Yan, M.; Jin, C.; Li, S. Characterization of Type-II Acetylated Cellulose Nanocrystals with Various Degree of Substitution and Its Compatibility in PLA Films. *Polymers* **2017**, *9*, No. 346.
(32) Semba, T.; Ito, A.; Kitagawa, K.; Kataoka, H.; Nakatsubo, F.; Kuboki, T.; Yano, H. Polyamide 6 composites reinforced with nanofibrillated cellulose formed during compounding: Effect of acetyl group degree of substitution. *Composites, Part A* **2021**, *145*, No. 106385.
(33) Hussain, R.; Batool, S. A.; Aizaz, A.; Abbas, M.; Ur Rehman, M. A. Biodegradable Packaging Based on Poly(vinyl Alcohol) and Carboxymethyl Cellulose Films Incorporated with Ascorbic Acid for Food Packaging Applications. *ACS Omega* **2023**, *8*, 42301−42310.
(34) Amorim, L. F. A.; Mouro, C.; Riool, M.; Gouveia, I. C. Antimicrobial Food Packaging Based on Prodigiosin-Incorporated Double-Layered Bacterial Cellulose and Chitosan Composites. *Polymers* **2022**, *14*, No. 315.
(35) Dairi, N.; Ferfera-Harrar, H.; Ramos, M.; Garrigós, M. C. Cellulose acetate/AgNPs-organoclay and/or thymol nano-biocomposite films with combined antimicrobial/antioxidant properties for active food packaging use. *Int. J. Biol. Macromol.* **2019**, *121*, 508−523.
(36) Ahmady, A. R.; Razmjooee, K.; Saber-Samandari, S.; Toghraie, D. Fabrication of chitosan-gelatin films incorporated with thymol-loaded alginate microparticles for controlled drug delivery, antibacterial activity and wound healing: In-vitro and in-vivo studies. *Int. J. Biol. Macromol.* **2022**, *223*, 567−582.
(37) Wen, Y.; Liu, J.; Jiang, L.; Zhu, Z.; He, S.; He, S.; Shao, W. Development of intelligent/active food packaging film based on TEMPO-oxidized bacterial cellulose containing thymol and anthocyanin-rich purple potato extract for shelf life extension of shrimp. *Food Packag. Shelf Life* **2021**, *29*, No. 100709.
(38) Nordin, N.; Othman, S. H.; Rashid, S. A.; Basha, R. K. Effects of glycerol and thymol on physical, mechanical, and thermal properties of corn starch films. *Food Hydrocolloids* **2020**, *106*, No. 105884.
(39) Chen, Y.; Qiu, Y.; Chen, W.; Wei, Q. Electrospun thymol-loaded porous cellulose acetate fibers with potential biomedical applications. *Mater. Sci. Eng.: C* **2020**, *109*, No. 110536.
(40) Kinnan, T.; Kondo, Y.; Aoki, M.; Inasawa, S. How do drying methods affect quality of films? Drying of polymer solutions under hot-air flow or infrared heating with comparable evaporation rates. *Drying Technol.* **2022**, *40*, 653−664.
(41) Yushkin, A. A.; Efimov, M. N.; Malakhov, A. O.; Karpacheva, G. P.; Bondarenko, G.; Marbelia, L.; Vankelecom, I. F. J.; Volkov, A. V. Creation of highly stable porous polyacrylonitrile membranes using infrared heating. *React. Funct. Polym.* **2021**, *158*, No. 104793.
(42) Chen, J. J.; Lin, J. D. Thermocapillary effect on drying of a polymer solution under non-uniform radiant heating. *Int. J. Heat Mass Transfer* **2000**, *43*, 2155−2175.
(43) Jo, C.; Rukmanikrishnan, B.; S, P. D.; Ramalingam, S.; Lee, J. Cellulose-Pulp-Based Stretchable Composite Film with Hydroxyethyl Cellulose and Turmeric Powder for Packaging Applications. *ACS Sustainable Chem. Eng.* **2021**, *9*, 13653−13662.
(44) Jo, C.; Kim, S. S.; Rukmanikrishnan, B.; Ramalingam, S.; S, P. D.; Lee, J. Properties of Cellulose Pulp and Polyurethane Composite Films Fabricated with Curcumin by Using NMMO Ionic Liquid. *Gels* **2022**, *8*, No. 248.
(45) Wang, L. Y.; Wang, M. J. Removal of Heavy Metal Ions by Poly(vinyl alcohol) and Carboxymethyl Cellulose Composite Hydrogels Prepared by a Freeze−Thaw Method. *ACS Sustainable Chem. Eng.* **2016**, *4*, 2830−2837.
(46) Ilyas, R. A.; Sapuan, S. M.; Ibrahim, R.; Abral, H.; Ishak, M. R.; Zainudin, E. S.; Atikah, M. S. N.; Nurazzi, N. M.; Atiqah, A.; Ansari, M. N. M.; Syafri, E.; Asrofi, M.; Sari, N. H.; Jumaidin, R. Effect of sugar palm nanofibrillated cellulose concentrations on morphological, mechanical and physical properties of biodegradable films based on

https://doi.org/10.1021/acsomega.4c03087
ACS Omega 2024, 9, 41258−41267

agro-waste sugar palm (Arenga pinnata (Wurmb.) Merr) starch. *J. Mater. Res. Technol.* **2019**, *8* (5), 4819−4830.
(47) Mastelić, J.; Jerković, I.; Blažević, I.; Poljak-Blaži, M.; Borović, S.; Ivančić-Baće, I.; Smrečki, V.; Žarković, N.; Brčić-Kostic, K.; Vikić-Topić, D.; Müller, N. Comparative Study on the Antioxidant and Biological Activities of Carvacrol, Thymol, and Eugenol Derivatives. *J. Agric. Food Chem.* **2008**, *56*, 3989−3996.
(48) Ramos, M.; Beltrán, A.; Peltzer, M.; Valente, A. J. M.; del Carmen Garrigós, M. Release and antioxidant activity of carvacrol and thymol from polypropylene active packaging films. *LWT−Food Sci. Technol.* **2014**, *58*, 470−477.

https://doi.org/10.1021/acsomega.4c03087
ACS Omega 2024, 9, 41258−41267